



Cite this: *Chem. Commun.*, 2016, 52, 11975

Received 11th July 2016,  
Accepted 7th September 2016

DOI: 10.1039/c6cc05705e

www.rsc.org/chemcomm

## Shape control of zincblende CdSe nanoplatelets†

Guillaume H. V. Bertrand,<sup>a</sup> Anatolii Polovitsyn,<sup>ab</sup> Sotirios Christodoulou,<sup>ab</sup>  
Ali Hossain Khan<sup>a</sup> and Iwan Moreels<sup>\*a</sup>

**The lateral dimensions of CdSe nanoplatelets have a strong and unique influence on their opto-electronic properties, with sizes that can be tuned from the weak to the strong exciton confinement regime. There are state-of-the-art reports on several nanoplatelet syntheses; however, at present only the thickness is well-controlled. We demonstrate here that we can achieve a control over the aspect ratio and overall nanoplate area by carefully adjusting the reagents that induce the in-plane growth. A variation of the fraction of hydrated Cd(OAc)<sub>2</sub> in a Cd(OAc)<sub>2</sub>/Cd(OAc)<sub>2</sub>·2H<sub>2</sub>O mixture tailors the nanoplatelet aspect ratio. This occurs independently of the reaction time, which can be used to fine-tune the overall length and width. An interpretation is given by the *in situ* formation of a small amount of hydroxide anions that alter the surface energy of specific planes.**

Understanding how size and shape influence the opto-electronic properties is an important topic in the field of colloidal nanocrystals (NCs). Control over the band structure is achieved most effectively by dedicated material design, for instance *via* growth of nanocrystals with spherical,<sup>1</sup> rod-,<sup>2</sup> or plate-like<sup>3</sup> geometry. The latter material class, labeled colloidal 2D nanoplatelets (NPLs), consists of NCs with a thickness of only a few atomic layers, typically around 4.5 monolayers (or about 1.4 nm).<sup>3,4</sup> This implies that they are substantially thinner than the bulk exciton Bohr diameter (11 nm), which brings the NPLs into the strong confinement regime along this direction. A comparatively large length and width typically yield only weak in-plane confinement for the 2D exciton.

The peculiar shape of NPLs implies specific advantages to engineer the opto-electronic properties. For example, it is well known that the band gap can be tuned – in discrete steps – by the NPL thickness, while at the same time the exciton lifetime is governed by the giant oscillator strength effect<sup>5–7</sup> that leads

to an exciton recombination rate scaling with the NPL area. Furthermore, the 2D shape enhances the linear<sup>8</sup> and nonlinear<sup>9</sup> absorption coefficients, and it enables an efficient suppression of nonradiative Auger recombination.<sup>10</sup> Recent experimental data have also shown that residual in-plane confinement effects in NPLs have a strong impact on exciton–phonon interactions and intraband carrier dynamics.<sup>11</sup> Next to the opto-electronic properties, shape and shape dispersion also play an important role in self-assembly<sup>12–14</sup> and the associated interparticle charge or energy transfer.

These results highlight the importance of shape- and area-controlled NPLs, yet the literature does not provide a general synthesis protocol that yields NPLs with tunable width and length. Published CdSe NPL shapes vary from elongated rectangles<sup>15</sup> to squares<sup>16</sup> and polygonal shapes,<sup>17</sup> and interestingly, protocols are all similar. However, previous work on the synthesis of shape-controlled nanocrystals has shown that small impurities can have profound effects. For instance, trace amounts of phosphonic acid in TOPO promoted rod-shaped NCs<sup>18</sup> and nanowires,<sup>19</sup> the addition of CdCl<sub>2</sub> to the CdSe synthesis can produce octapods,<sup>20</sup> or lead acetate impurities in lead oleate caused PbSe NCs to grow as hexagonal stars.<sup>21</sup>

In this communication we focus our synthetic efforts on controlling the aspect ratio (AR) of CdSe NPLs by careful examination of the different short-chained reactants that induce lateral growth.<sup>22,23</sup> We will show that the AR of CdSe NPLs depends on the presence of water in the cadmium-acetate precursor, with further experiments pointing toward the *in situ* formation of hydroxide anions. This implies that carefully adjusted mixtures of short-chained Cd-precursors allow for a tuning of the AR in a range from square NPLs (AR 1 : 1) to highly elongated rectangles (AR 8 : 1). In combination with a size-controlled NPL synthesis by adjusting the reaction time, the NPL width can be tuned from 15 nm down to 2.4 nm, leading to a shift in band edge absorption (emission) from 513 nm (515 nm) to 498 nm (502 nm).

It is well known that injection of cadmium acetate (Cd(OAc)<sub>2</sub>), cadmium acetate dihydrate (Cd(OAc)<sub>2</sub>·2H<sub>2</sub>O) or cadmium propionate (Cd(OPr)<sub>2</sub>) triggers the lateral growth of NPLs. Depending on

<sup>a</sup> Istituto Italiano di Tecnologia, via Morego 30, IT-16163 Genova, Italy.  
E-mail: iwan.moreels@iit.it

<sup>b</sup> Dipartimento di Fisica, Università di Genova, Via Dodecaneso 33,  
IT-16146 Genova, Italy

† Electronic supplementary information (ESI) available: Synthesis details and thermogravimetric analysis of the precursors, NPL control experiments, X-ray diffraction patterns and size-dependent optical properties. See DOI: 10.1039/c6cc05705e



the protocol, the resulting platelet shape varied from rectangular<sup>15</sup> to square<sup>16</sup> or polygonal.<sup>17</sup> Here, we performed a typical CdSe NPL synthesis with the injection of dry  $\text{Cd}(\text{OAc})_2$ . In a 50 mL three neck round bottom flask 150 mg of dry cadmium myristate ( $\text{Cd}(\text{Myr})_2$ , 0.26 mmol, the absence of water was verified using thermo-gravimetric analysis, TGA, see the ESI†), 24 mg of selenium (Se) powder (0.30 mmol) and 15 mL of octadecene (ODE) were degassed under vacuum at 110 °C for 20 min. The mixture was placed under an argon atmosphere and heated to 140 °C for 10 to 20 minutes to achieve total Se dissolution. The temperature was then set to 240 °C with a ramp of 50 °C min<sup>-1</sup>. Between 205 °C and 215 °C the solution changed color from yellow to deep orange, at which point the reaction vessel was opened and 80 mg of dry  $\text{Cd}(\text{OAc})_2$  (0.35 mmol) was added. When the solution reached 240 °C, the NPLs were grown for 8 min, after which the heating mantle was removed, the reaction mixture was slowly cooled to 160 °C, and 2 mL of oleic acid was added. When reaching room temperature, 20 mL of hexane was added and the solution was centrifuged for 10 min at 3000 rpm. The supernatant was discarded and the precipitate was dispersed in 40 mL of hexane. The resulting solution was centrifuged again at 6000 rpm. The desired NPLs remained in the supernatant and the precipitate was discarded.

To record bright-field transmission electron microscopy (TEM) images, a few drops of a diluted NPL suspension in hexane were dropped on a TEM grid (E.M. Sciences, a carbon film on a 300 mesh copper grid) and inserted into a JEM 1011 electron microscope. Fig. 1a shows the result of a typical synthesis using dry  $\text{Cd}(\text{OAc})_2$ . We obtained NPLs with an AR of 7.5:1 and an average width of 6.8 nm (ESI†, Table S1). We also evaluated the influence of the different reagents ( $\text{Cd}(\text{Myr})_2$ ,  $\text{Cd}(\text{OAc})_2$ , Se) for this reaction, however, the use of different concentrations of each component has no significant influence on the final AR (ESI†, Tables S2–S4). In strong contrast, upon replacing dry  $\text{Cd}(\text{OAc})_2$  by an equimolar amount of  $\text{Cd}(\text{OAc})_2 \cdot 2\text{H}_2\text{O}$  and applying the same synthesis procedure as above, a distinctively different shape was observed (Fig. 1b, ESI†, Table S1). While the first precursor leads to highly rectangular NPLs, laterally terminated by (100) and (010) facets,<sup>22</sup> the latter yields more irregular shapes with a lower AR of 2.3:1, with the appearance of (110) facets. For obtaining the latter NPLs, the importance of having traces of water present was confirmed by a control experiment where we co-injected 20  $\mu\text{L}$  of water together with dry  $\text{Cd}(\text{OAc})_2$  in an ODE solution containing the CdSe seeds at 210 °C. Despite a rapid vapor development that suggested some loss of water, enough remained to again afford polygonal platelets with an AR of 1.2:1 and an average width and length of 13.7 nm and 16.3 nm, resp. (Fig. 1c).

It is clear that water plays an important role in the AR-control of CdSe NPLs. In the literature, trace amounts of water or hydroxide anions have led to a hindered growth of InP quantum dots,<sup>24</sup> and hydroxide anions are also known to bind to and passivate specific facets of PbS NCs.<sup>25</sup> We therefore postulate that here also the active species is a hydroxide anion that can adsorb and alter the surface energy balance, and therefore lead to a different shape by modifying the growth rate of specific

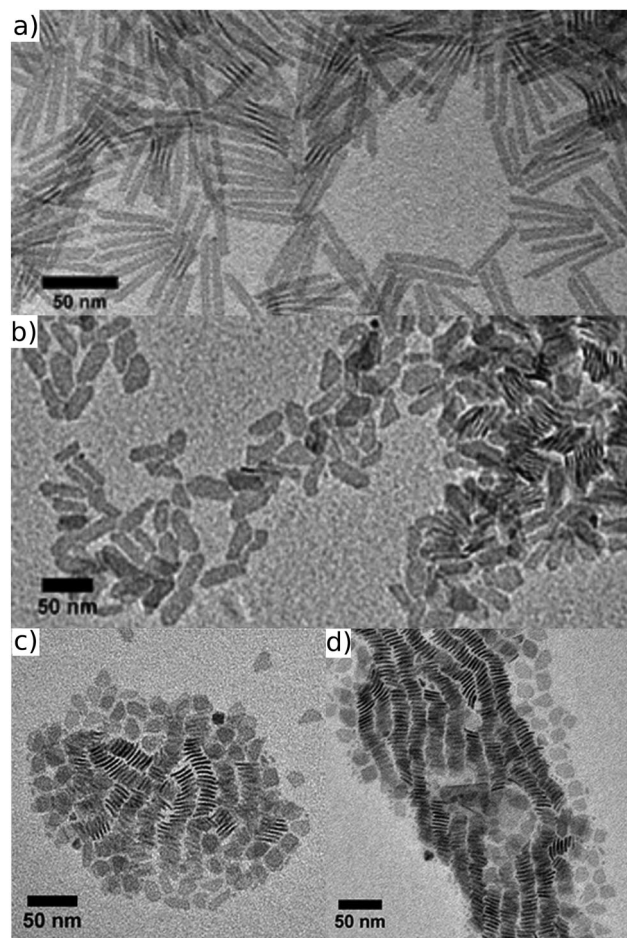
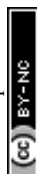


Fig. 1 (a) TEM image of 4.5 mL of CdSe NPLs synthesized using dry  $\text{Cd}(\text{OAc})_2$ . (b) TEM image of 4.5 mL of CdSe NPLs synthesized using  $\text{Cd}(\text{OAc})_2 \cdot 2\text{H}_2\text{O}$ . (c) TEM image of 4.5 mL of CdSe NPLs synthesized using dry  $\text{Cd}(\text{OAc})_2$  and 20  $\mu\text{L}$  of water. (d) TEM image of 4.5 mL of CdSe NPLs synthesized using 93 mol% dry  $\text{Cd}(\text{OAc})_2$  and 7 mol%  $\text{Cd}(\text{OH})_2$ .

facets according to the model recently proposed by Riedinger *et al.*<sup>26</sup> To validate the presence of  $\text{OH}^-$  and its effect on the growth, we performed a synthesis where a small fraction of dry  $\text{Cd}(\text{OAc})_2$  was replaced by dry  $\text{Cd}(\text{OH})_2$  (the absence of water was verified by TGA, see the ESI†). A clear modification of the AR was observed, even with small inclusions of  $\text{OH}^-$  (Fig. 1d). We were able to tune the NPL AR from rectangles with an AR of 7.7:1 to almost square NPLs with AR 1.3:1 by controlling the fraction of  $\text{Cd}(\text{OH})_2$  between 0 and 7 mol% (ESI†, Table S5). Note that X-ray diffraction patterns confirm that the use of either dry or hydrated  $\text{Cd}(\text{OAc})_2$ , as well as inclusion of  $\text{Cd}(\text{OH})_2$  in the synthesis, all lead to NPLs with a zincblende lattice structure (ESI†, Section S4).

The results thus suggest that upon injection of  $\text{Cd}(\text{OAc})_2 \cdot 2\text{H}_2\text{O}$  at 210 °C in ODE, the majority of water may evaporate, but a small part reacts with the acetate ligands to create hydroxide anions and acetic acid, which subsequently leads to a reduced AR during NPL growth. However, considering that only a small amount (*ca.* 7 mol%) of  $\text{Cd}(\text{OH})_2$  was needed to achieve square NPLs, the use of  $\text{Cd}(\text{OAc})_2 \cdot 2\text{H}_2\text{O}$  actually represents a more convenient route to tune the AR, as it can



**Table 1** Synthesis of NPLs with different wet/dry Cd(OAc)<sub>2</sub> ratios

Name	Cd(OAc) <sub>2</sub> (mol%)	Cd(OAc) <sub>2</sub> ·2(H <sub>2</sub> O) (mol%)	Length (nm)	Width (nm)	Ratio
NPL-1	100	0	40.38	5.34	7.67
NPL-2	95	5	33.16	5.11	6.58
NPL-3	90	10	52.98	9.44	5.66
NPL-4	80	20	38.66	8.94	4.39
NPL-5	75	25	33.86	8.58	4
NPL-6	70	30	37.88	10.97	3.51
NPL-7	60	40	16.77	8.17	2.10
NPL-8	50	50	17.32	9.97	1.77
NPL-9	40	60	13.88	10.36	1.34
NPL-10	30	70	17.62	15.22	1.17
NPL-11	20	80	20.09	13.64	1.47
NPL-12	10	90	21.04	15.14	1.40
NPL-13	0	100	34.20	14.90	2.30

rely on the *in situ* generation of hydroxide anions. To verify this approach, different ratios of dry and hydrated cadmium acetate were used while maintaining a fixed total amount of cadmium

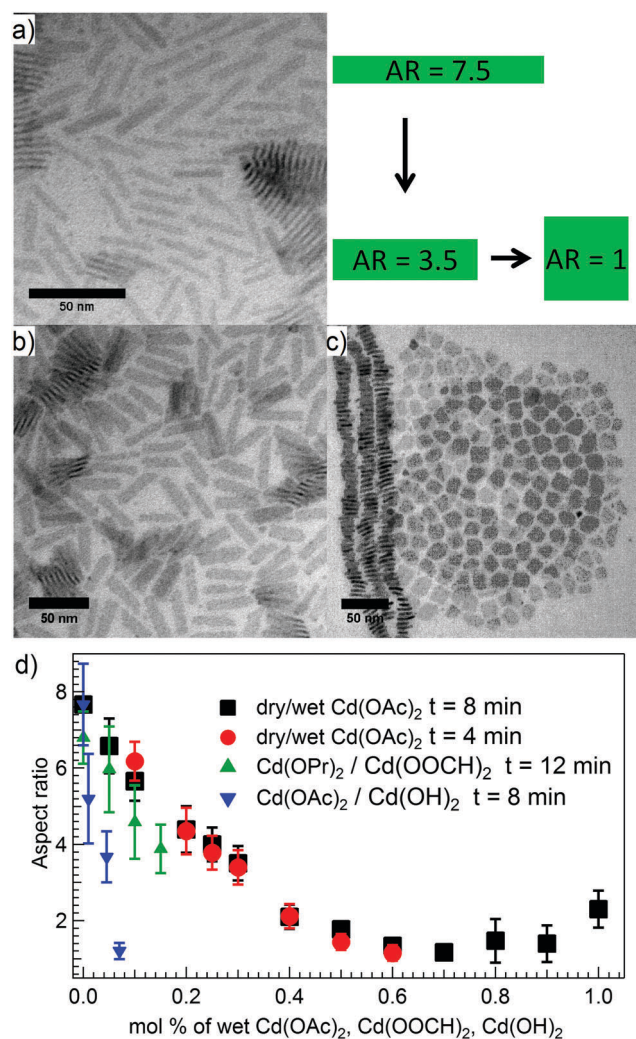


**Fig. 2** TEM images of samples (a) NPL-1, (b) NPL-6, (c) and NPL-10 illustrating the aspect ratio control. (d) Plot of the CdSe NPL aspect ratio versus the molar percentage of Cd(OAc)<sub>2</sub>·2H<sub>2</sub>O, Cd(OOCH)<sub>2</sub>, and Cd(OH)<sub>2</sub> precursors, respectively.

(Table 1). The AR could be tuned continuously from 7.7:1 for dry Cd(OAc)<sub>2</sub> to square NPLs for a mixture of 30 mol% dry Cd(OAc)<sub>2</sub> and 70 mol% Cd(OAc)<sub>2</sub>·2H<sub>2</sub>O (Fig. 2). A similar curve is obtained when reducing the growth to 4 minutes (Fig. 2c, ESI†, Table S6), which attests that the AR is independent of the reaction time. Note that above 70 mol% of Cd(OAc)<sub>2</sub>·2H<sub>2</sub>O, the AR increases again, however, this is in the range where we obtained polygon-shaped particles instead of rectangular NPLs (note that the lower AR limit is 1:1 by definition as we place the shorter dimension in the denominator).

The tuning can be expanded to other combinations of short-chained precursors as well. We found that for reactions using dry Cd(OPr)<sub>2</sub> (see the ESI† for TGA data), the addition of small amounts of cadmium formate (Cd(OOCH)<sub>2</sub>) yielded a similar AR control (ESI†, Table S7). This suggests that OOCCH<sup>−</sup> ions afford an alternative to the AR-tuning *via* OH<sup>−</sup> ions. We obtained NPLs with an AR varying from 6.5:1 with dry Cd(OPr)<sub>2</sub>, to 3.8:1 when the fraction of Cd(OOCH)<sub>2</sub> was increased to 15 mol%. However, when using amounts of Cd(OOCH)<sub>2</sub> superior to 20 mol% we observed a 3D growth of spherical nanocrystals; hence, we were not able to obtain square NPLs with Cd(OOCH)<sub>2</sub>.

As the AR increases, typically the NPL width is reduced. Consequently, the optical properties and more specifically the band-edge absorption and fluorescence can be precisely tuned by controlling the AR. To measure the optical properties, a diluted NPL suspension in hexane was added to a 3 mL quartz

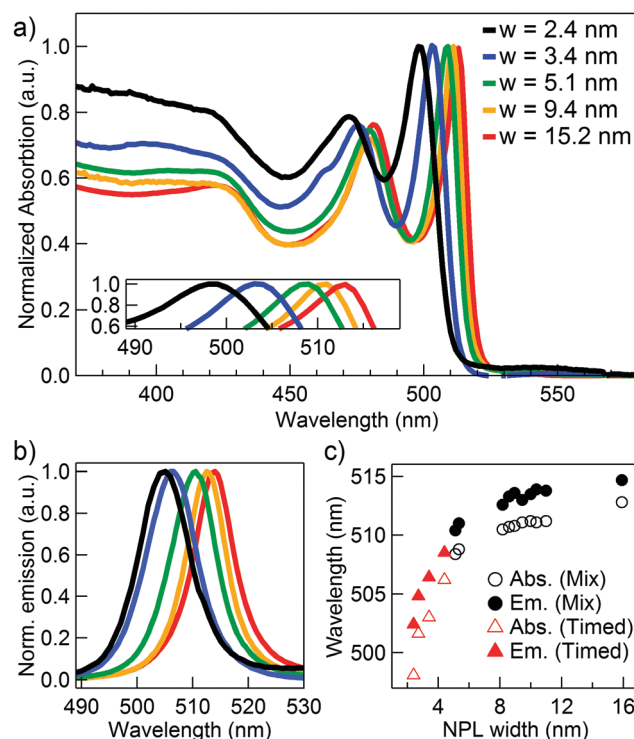


**Fig. 3** (a) Absorption spectra of NPLs with different widths. (b) Corresponding NPL emission spectra. (c) Maxima of first absorption (open symbols) and emission (closed symbols) peaks plotted against NPL width. The width was tuned either by adjusting the reaction time (1.5 min to 4 min, triangles), or using dry/wet Cd(OAc)<sub>2</sub> mixtures (0–70 mol%, circles).



cuvette. Absorbance spectra were collected using a Cary 300 scan Varian spectrometer. Fluorescence spectra were recorded using an Edinburgh Instruments FLS920 spectrofluorimeter. We observed that the absorption and emission maxima progressively blue shifted with decreasing width (Fig. 3, ESI,† Table S10). Using an 8 minute reaction time, the absorption (fluorescence) maximum could be varied from 512.8 nm (514.7 nm) for 15.2 nm wide NPLs, to 508.4 nm (510.4 nm) when the width was reduced to 5.1 nm. Since dry Cd(OAc)<sub>2</sub> yielded the narrowest NPLs, a further reduction could be achieved by reducing the reaction time (ESI,† Table S8), blue shifting the band-edge optical properties further to an absorption (emission) maximum of 498.1 nm (502.4 nm). With a final width of the smallest sample of only 2.4 nm, the synthesis thus allows tuning the particle properties continuously from the weak to the strong lateral confinement regime. These NPLs should therefore also be highly suitable for further studies on the role of quantum confinement in colloidal (quasi-)2D nanostructures.

In conclusion, we described a synthesis protocol that allows tuning of the aspect ratio of zincblende CdSe NPLs, *via* a precise control of the ratio of dry to hydrated cadmium acetate. We demonstrated how to gain access to a family of CdSe NPLs of different rectangular shapes with areas between 15 and 500 nm<sup>2</sup> and ARs between 1 : 1 and 7.7 : 1. The role of the OH<sup>−</sup> moiety was crucial in the growth of shape-controlled NPLs, as a competitive 2D growth agent next to Cd(OAc)<sub>2</sub>. Through the NPL shape and overall area, a targeted tuning of the absorption and emission properties is now possible.

The present publication was realized with the support of the Ministero degli Affari Esteri e della Cooperazione Internazionale (IONX-NC4SOL). The authors thank G. Pugliese for measuring the TGA data.

## Notes and references

- 1 J. Park, J. Joo, G. K. Soon, Y. Jang and T. Hyeon, *Angew. Chem., Int. Ed.*, 2007, **46**, 4630–4660.
- 2 A. Wolcott, R. C. Fitzmorris, O. Muzaffery and J. Z. Zhang, *Chem. Mater.*, 2010, **22**, 2814–2821.
- 3 S. Ithurria and B. Dubertret, *J. Am. Chem. Soc.*, 2008, **130**, 16504–16505.
- 4 S. Ithurria and D. V. Talapin, *J. Am. Chem. Soc.*, 2012, **134**, 18585–18590.
- 5 S. Ithurria, M. D. Tessier, B. Mahler, R. P. S. M. Lobo, B. Dubertret and A. L. Efros, *Nat. Mater.*, 2011, **10**, 936–941.
- 6 A. W. Achtstein, A. Schliwa, A. Prudnikau, M. Hardzei, M. V. Artemyev, C. Thomsen and U. Woggon, *Nano Lett.*, 2012, **12**, 3151–3157.
- 7 A. Naeem, F. Masia, S. Christodoulou, I. Moreels, P. Borri and W. Langbein, *Phys. Rev. B*, 2015, **91**, 121302(R).
- 8 A. W. Achtstein, A. Antanovich, A. Prudnikau, R. Scott, U. Woggon and M. Artemyev, *J. Phys. Chem. C*, 2015, **119**, 20156–20161.
- 9 R. Scott, A. W. Achtstein, A. Prudnikau, A. Antanovich, S. Christodoulou, I. Moreels, M. Artemyev and U. Woggon, *Nano Lett.*, 2015, **15**, 4985–4992.
- 10 L. T. Kunneman, M. D. Tessier, H. Heuclin, B. Dubertret, Y. V. Aulin, F. C. Grozema, J. M. Schins and L. D. A. Siebbeles, *J. Phys. Chem. Lett.*, 2013, **4**, 3574–3578.
- 11 A. W. Achtstein, R. Scott, S. Kickhöfel, S. T. Jagsch, S. Christodoulou, G. H. V. Bertrand, A. V. Prudnikau, A. Antanovich, M. Artemyev, I. Moreels, A. Schliwa and U. Woggon, *Phys. Rev. Lett.*, 2016, **116**, 116802.
- 12 B. Guzelturk, M. Olutas, S. Delikanli, Y. Kelestemur, O. Erdem and H. V. Demir, *Nanoscale*, 2015, **7**, 2545–2551.
- 13 C. E. Rowland, I. Fedin, H. Zhang, S. K. Gray, A. O. Govorov, D. V. Talapin and R. D. Schaller, *Nat. Mater.*, 2015, **14**, 484–489.
- 14 S. Jana, T. N. T. Phan, C. Bouet, M. D. Tessier, P. Davidson, B. Dubertret and B. Abécassis, *Langmuir*, 2015, **31**, 10532–10539.
- 15 E. Lhuillier, P. Hease, S. Ithurria and B. Dubertret, *Chem. Mater.*, 2014, **26**, 4514–4520.
- 16 B. Abécassis, M. D. Tessier, P. Davidson and B. Dubertret, *Nano Lett.*, 2014, **14**, 710–715.
- 17 S. Pedetti, S. Ithurria, H. Heuclin, G. Patriarche and B. Dubertret, *J. Am. Chem. Soc.*, 2014, **136**, 16430–16438.
- 18 X. G. Peng, L. Manna, W. D. Yang, J. Wickham, E. Scher, A. Kadavanich and A. P. Alivisatos, *Nature*, 2000, **404**, 59–61.
- 19 F. Wang, R. Tang and W. E. Buhro, *Nano Lett.*, 2008, **8**, 3521–3524.
- 20 M. R. Kim, K. Miszt, M. Povia, R. Brescia, S. Christodoulou, M. Prato, S. Marras and L. Manna, *ACS Nano*, 2012, **6**, 11088–11096.
- 21 A. J. Houtepen, R. Koole, D. Vanmaekelbergh, J. Meeldijk and S. G. Hickey, *J. Am. Chem. Soc.*, 2006, **128**, 6792–6793.
- 22 S. Ithurria, G. Bousquet and B. Dubertret, *J. Am. Chem. Soc.*, 2011, **133**, 3070–3077.
- 23 C. Bouet, B. Mahler, B. Nadal, B. Abecassis, M. D. Tessier, S. Ithurria, X. Xu and B. Dubertret, *Chem. Mater.*, 2013, **25**, 639–645.
- 24 L. Xie, D. K. Harris, M. G. Bawendi and K. F. Jensen, *Chem. Mater.*, 2015, **27**, 5058–5063.
- 25 D. Zherebetskyy, M. Scheele, Y. Zhang, N. Bronstein, C. Thompson, D. Britt, M. Salmeron, P. Alivisatos and L. W. Wang, *Science*, 2014, **344**, 1380–1384.
- 26 A. Riedinger, F. D. Ott, A. Mule, S. Mazzotti, P. N. Knüsel, S. J. P. Kress, F. Prins, S. C. Erwin, D. J. Norris, 2016, ArXiv:1605.06553.

